

The Standard Model (SM) [1] is a name given in the 1970s to a theory describing the fundamental particles and their interactions. This quantum field theory describes the particles and their interactions as fields and has successfully incorporated three of the four fundamental forces in the universe. In Section 1.1, the particle content of the SM is summarised, while Section 1.2 describes the SM Lagrangian and its symmetries. In Section 1.3, the flavour content of the SM is highlighted, and Section 1.4 focusses on the top quark in the SM.

The successful theory of the SM has some shortcomings which are discussed in Section 1.6 and lead to searches for a more general theory. One of such is using an effective field theory (EFT) approach [2] to search for new physics in a model independent way. In Section 1.7 an EFT model focussing on flavour changing neutral currents (FCNC) involving a top quark is presented. Its current experimental constraints are given in Section 1.8.

1.1 Elementary particles and forces

The interactions in nature can be described by four forces, the strong force, the electromagnetic (EM) force, the weak force and the gravitational force. These interactions happen via particles with an integer spin known as bosons. The strong interaction is mediated by eight gluons g , while the electromagnetic force is mediated by photons γ , and the weak force by Z and W^\pm bosons. In Table 1.1, the forces and their characteristics are shown. The gravitational force is the only force not included in the SM and can be neglected for energies lower than the Planck scale (1.22×10^{19} GeV).

Table 1.1: The four forces of nature and their characteristics.

	Range	Mediator
Strong force	10^{-15} m	8 gluons
Electromagnetic force	∞	photon
Weak force	10^{-18} m	W^\pm , Zbosons
Gravitational force	∞	unknown

The fermions are the particles that make up the visible matter in the universe. They carry half integer spin and can be subdivided into leptons and quarks, where leptons do not interact strongly. Each fermion has a corresponding anti-fermion which has the same mass and is oppositely charged. The electron e is the first elementary particle discovered [3] and belongs to the first generation of leptons together with the electron neutrino ν_e . The second generation comprises the muon μ and muon neutrino ν_μ , whereas the third generation consists of the tau τ and tau neutrino ν_τ . The neutrinos are neutral particles, while the other leptons have charge $\pm q_e$ with q_e representing the elementary charge of 1.602×10^{-19} C. The masses of charged leptons differ by four orders of magnitude between the first and third generations. In the SM the neutrinos are assumed to be massless, nonetheless it is experimentally established that neutrinos do have a tiny non-zero mass [4, 5]. In Table 1.2, the leptons and their properties in the SM are summarised.

Table 1.2: The properties of the leptons in the three generations of the SM [6], where q_e represents the elementary charge.

Generation	Particle	Mass	Charge
First	e^-	0.511 MeV	$-q_e$
	ν_e	≈ 0	0
Second	μ^-	106 MeV	$-q_e$
	ν_μ	≈ 0	0
Third	τ^-	1 777 MeV	$-q_e$
	ν_τ	≈ 0	0

The quarks can also be divided into three generations. Unlike the leptons, they carry colour charge and can interact via the strong interaction. The top quark, discovered in 1995 at the Tevatron [7, 8], is the heaviest SM particle with a mass¹ measured to be $173.34 \pm 0.27(\text{stat}) \pm 0.71(\text{syst})$ GeV [9]. The quarks and their properties are summarised in Table 1.3. In nature, only colour neutral objects can exist. This has as consequence that quarks are bound through gluons into mesons (quark+anti-quark) and baryons (three quarks). These mesons and baryons are mostly short-lived and unstable particles that rapidly decay through W^\pm and Z bosons. The only known stable baryon is the proton, made up of two up quarks and one down quark.

The scalar boson, commonly known as the Higgs boson, is the last piece of the SM discovered in 2012 [10, 11]. It is responsible for the masses of the W^\pm and Z boson, and that of the fermions.

¹In this thesis all masses and energies are expressed in natural units, where the speed of light and \hbar are taken to be equal to one.

Table 1.3: The properties of the quarks in the three generations of the SM [6], where q_e represents the elementary charge.

Generation	Particle	Mass	Charge
First	up u	$2.2^{+0.6}_{-0.4}$ MeV	$\frac{2}{3} q_e$
	down d	$4.7^{+0.5}_{-0.4}$ MeV	$\frac{1}{3} q_e$
Second	charm c	1.28 ± 0.03 GeV	$\frac{2}{3} q_e$
	strange s	96^{+8}_{-4} MeV	$\frac{1}{3} q_e$
Third	top t	173.1 ± 0.6 GeV	$\frac{2}{3} q_e$
	bottom b	$4.18^{+0.04}_{-0.03}$ GeV	$\frac{1}{3} q_e$

1.2 Standard Model Lagrangian, connecting fields with particles

The SM is a quantum field theory and thus describes the dynamics and kinematics of particles and forces by a Lagrangian \mathcal{L} . The theory is based on the $SU(3)_C \times SU(2)_L \times U(1)_Y$ gauge symmetry, where $SU(2)_L \times U(1)_Y$ describes the electroweak interaction and $SU(3)_C$ the strong interaction. The indices refer to colour C, the left chiral nature of the $SU(2)_L$ coupling L, and the weak hypercharge Y. Its Lagrangian is constructed such that symmetries representing physics conservation laws such as conservation of energy, momentum and angular momentum are contained. The symmetries under local gauge transformations are sustained by demanding gauge invariance².

The $U(1)_Y$ group has one generator Y with an associated gauge field B_μ . The three gauge fields W_μ^1 , W_μ^2 , and W_μ^3 , are associated to $SU(2)_L$ with three generators that can be written as half of the Pauli matrices:

$$T_1 = \frac{1}{2} \begin{pmatrix} 0 & 1 \\ 1 & 0 \end{pmatrix}, T_2 = \frac{1}{2} \begin{pmatrix} 0 & -i \\ i & 0 \end{pmatrix}, \text{ and } T_3 = \frac{1}{2} \begin{pmatrix} 1 & 0 \\ 0 & -1 \end{pmatrix}. \quad (1.1)$$

The generators T^a satisfy the Lie algebra:

$$[T_a, T_b] = i\epsilon_{abc} T^c \text{ and } [T_a, Y] = 0, \quad (1.2)$$

where ϵ_{abc} is an antisymmetric tensor. The gauge fields of $SU(2)_L$ only couple to left-handed fermions as required by the observed parity violating nature of the weak force. The $SU(3)_C$ group represents quantum chromodynamics (QCD). It has eight generators corresponding to eight gluon fields $G_\mu^{1\dots 8}$. Unlike $SU(2)_L \times U(1)_Y$, $SU(3)_C$ is not chiral.

Under $SU(3)_C$ quarks are colour triplets while leptons are colour singlets. This implies that the quarks carry a colour index ranging between one and three, whereas leptons do not take part in strong interactions. Based on the chirality, the quarks and leptons are organized in doublets or singlets. Each generation i of fermions consists of left-handed doublets and right-handed

²Different field configurations of unobservable fields can result in identical quantities. Transformations between such configurations are called gauge transformation and the absence of change in the measurable quantities is a characteristic called gauge invariance.

singlets:

$$l_{L,i} = \begin{pmatrix} e_{L,i} \\ \nu_{L,i} \end{pmatrix}, e_{R,i}, q_{L,i} = \begin{pmatrix} u_{L,i} \\ d_{L,i} \end{pmatrix}, u_{R,i}, \text{ and } d_{R,i} \quad (1.3)$$

The SM Lagrangian can be decomposed as a sum of four terms

$$\mathcal{L}_{\text{SM}} = \mathcal{L}_{\text{gauge}} + \mathcal{L}_f + \mathcal{L}_{\text{Yuk}} + \mathcal{L}_\phi, \quad (1.4)$$

that are related to the gauge, fermion, Yukawa and scalar sectors. The gauge Lagrangian regroups the gauge fields of all three symmetry groups, and the fermionic part consists of kinetic energy terms for quarks and leptons. The interaction between fermions and the scalar doublet ϕ gives rise to fermion masses and is described by the Yukawa Lagrangian. The scalar part of the Lagrangian is composed of a kinematic and potential component related to the scalar boson.

For the electroweak theory, two coupling constants are introduced, namely g' for $U(1)_Y$ and g for $SU(2)_L$. The physically observable gauge bosons of this theory are the photon field A_μ , the Z boson field Z_μ^0 , and the W boson fields W_μ^\pm . These are a superposition of the four gauge fields of $SU(2)_L \times U(1)_Y$:

$$\begin{aligned} A_\mu &= \sin \theta_W W_\mu^3 + \cos \theta_W B_\mu, \\ Z_\mu^0 &= \cos \theta_W W_\mu^3 - \sin \theta_W B_\mu, \text{ and} \\ W_\mu^\pm &= \sqrt{\frac{1}{2}} (W_\mu^1 \mp i W_\mu^2), \end{aligned} \quad (1.5)$$

where θ_W represents the weak mixing angle defined as $\tan \theta_W = \frac{g'}{g}$.

The coupling constant representing the strength of the QCD interactions is denoted as g_s . In QCD there is asymptotic freedom whereby the strong coupling constant becomes weaker as the energy with which the interaction between strongly interacting particles is probed increases, and stronger as the distance between the particles increases. A consequence of this is known as colour confinement, the quarks and gluons can not exist on their own and are not observed individually. They are bound in colour neutral states called hadrons, this process is known as hadronisation.

Electroweak symmetry breaking

In $\mathcal{L}_{\text{gauge}}$ and \mathcal{L}_f are no mass terms for fermions present because only singlets under $SU(3)_C \times SU(2)_L \times U(1)_Y$ can acquire a mass with an interaction of the type $m^2 \phi^\dagger \phi$ without breaking the gauge invariance. In order to accommodate mass terms for fermions and gauge fields, electroweak symmetry breaking, leading to \mathcal{L}_ϕ is introduced.

The scalar doublet is introduced in the SM as

$$\phi = \frac{1}{\sqrt{2}} \begin{pmatrix} \varphi_1 + i\varphi_2 \\ \varphi_3 + i\varphi_4 \end{pmatrix}. \quad (1.6)$$

Its field potential is of the form

$$V(\phi) = \mu^2 \phi^\dagger \phi + \lambda (\phi^\dagger \phi)^2, \quad (1.7)$$

with $\mu^2 < 0$ and λ a positive integer. This choice of parameters gives the potential a "Mexican hat" shape. It has an infinite set of minima (ground states) and by expanding the field around an arbitrary choice of ground state, the electroweak symmetry is broken (EW):

$$\phi = \begin{pmatrix} 0 \\ \frac{v}{\sqrt{2}} \end{pmatrix} + \hat{\phi}, \quad (1.8)$$

where v is the vacuum expectation value (vev), measured to be around 245 GeV and corresponds to $\sqrt{\frac{-\mu}{\lambda}}$. The scalar doublet's four degrees of freedom are reduced to three degrees of freedom that couple to the gauge fields and fix the W^+ , W^- and Zbosons. The remaining fourth degree of freedom has given rise to a physically observable particle, called the Brout-Englert-Higgs (BEH) boson. This spontaneous symmetry breaking leaves the gauge invariance intact and gives masses to the W^\pm and Zbosons as:

$$m_W = \frac{1}{2} v |g| \quad \text{and} \quad m_Z = \frac{1}{2} v \sqrt{g'^2 + g^2}. \quad (1.9)$$

170 The Brout-Englert-Higgs field couples universally to fermions with a strength proportional to
171 their masses, and to gauge bosons with a strength proportional to the square of their masses.

172 1.3 Flavours in the SM

Flavour changing charged currents are introduced in 1963 by Nicola Cabibbo [12]. Via interactions with a W boson the flavour of the quarks is changed. At the time of the postulation only up, down, and strange quarks were known and the charged weak current was described as a coupling between the up quark and d_{weak} , where d_{weak} is a linear combination of the down and strange quarks, $d_{\text{weak}} = \cos\theta_c d + \sin\theta_c s$. This linear combination is a direct consequence of the chosen rotation

$$\begin{pmatrix} d_{\text{weak}} \\ s_{\text{weak}} \end{pmatrix} = \begin{pmatrix} \cos\theta_c & \sin\theta_c \\ -\sin\theta_c & \cos\theta_c \end{pmatrix} \begin{pmatrix} d \\ s \end{pmatrix} = \mathcal{R} \begin{pmatrix} d \\ s \end{pmatrix}, \quad (1.10)$$

where the rotation angle θ_c is known as the Cabibbo angle. This provides a definition for the charged weak current between u and d quarks,

$$J_\mu = \bar{u} \gamma_\mu (1 + \gamma_5) d_{\text{weak}}. \quad (1.11)$$

A consequence of Cabibbo's approach is that the s_{weak} is left uncoupled, leading to Glashow, Iliopoulos and Maiani (GIM) [13–15] to require the existence of a fourth quark with charge $\frac{2}{3}q_e$. This quark, known as the charm quark, couples to s_{weak} and a new definition of the charged weak current is modified to

$$J_\mu = (\bar{u} \quad \bar{c}) \gamma_\mu (1 + \gamma_5) \mathcal{R} \begin{pmatrix} d \\ s \end{pmatrix} = \bar{U} \gamma_\mu (1 + \gamma_5) \mathcal{R} D. \quad (1.12)$$

The neutral weak current is defined as

$$J_3 = \bar{U} \gamma_\mu (1 + \gamma_5) [\mathcal{R}, \mathcal{R}^\dagger] D, \quad (1.13)$$

and is diagonal in flavour space. This has as consequence that no flavour changing neutral currents occur at tree-level interactions [1].

Kobayashi and Maskawa generalised the Cabibbo rotation matrix to accommodate a third generation of quarks. The result is a 3×3 unitary matrix known as the CKM matrix, responsible for the mixing of weak interaction states of down-type quarks:

$$\begin{pmatrix} d_{\text{weak}} \\ s_{\text{weak}} \\ b_{\text{weak}} \end{pmatrix} = \begin{pmatrix} V_{ud} & V_{us} & V_{ub} \\ V_{cd} & V_{cs} & V_{cb} \\ V_{td} & V_{ts} & V_{tb} \end{pmatrix} \begin{pmatrix} d \\ s \\ b \end{pmatrix} = \mathcal{V}_{\text{CKM}} \begin{pmatrix} d \\ s \\ b \end{pmatrix}, \quad (1.14)$$

where \mathcal{V}_{CKM} is unitary ($\mathcal{V}_{\text{CKM}}^\dagger \mathcal{V}_{\text{CKM}} = \mathbb{1}$). A general 3×3 unitary matrix depends on three real angles and six phases. For the CKM matrix, the freedom to redefine the phases of the quark eigenstates can remove five of the phases, leaving a single physical phase known as the Kobayashi-Maskawa phase. This phase is responsible for the charge parity violation in the SM [16]. Each element V_{ij} of \mathcal{V}_{CKM} represents the transition probability of a quark i going to a quark j , and is experimentally determined to be [6]

$$\mathcal{V}_{\text{CKM}} = \begin{pmatrix} 0.97425 \pm 0.00022 & 0.2253 \pm 0.0008 & (4.13 \pm 0.49) \times 10^{-3} \\ 0.225 \pm 0.008 & 0.986 \pm 0.016 & (41.1 \pm 1.3) \times 10^{-3} \\ (8.4 \pm 0.6) \times 10^{-3} & (40.0 \pm 2.7) \times 10^{-3} & 1.021 \pm 0.032 \end{pmatrix}. \quad (1.15)$$

From Equation 1.15 follows that top quarks predominantly decay via charged weak currents to bottom quarks, with a probability consistent with unity. In the SM, FCNC can only occur via higher loop interactions which are highly suppressed. The expected transition probabilities for a top quark decaying via a FCNC interaction in the SM are given in Table 1.4, where it is clear that the FCNC top quark interactions of the SM is still beyond the reach of the sensitivity of current experiments.

Table 1.4: The predicted branching fractions \mathcal{B} for FCNC decays involving the top quark in the SM [17].

Process	\mathcal{B} in the SM	Process	\mathcal{B} in the SM
$t \rightarrow uZ$	8×10^{-17}	$t \rightarrow cZ$	1×10^{-14}
$t \rightarrow u\gamma$	4×10^{-16}	$t \rightarrow c\gamma$	5×10^{-14}
$t \rightarrow ug$	4×10^{-14}	$t \rightarrow cg$	5×10^{-12}
$t \rightarrow uH$	2×10^{-17}	$t \rightarrow cH$	3×10^{-15}

180

1.4 The top quark in the SM

181

Discovered in 1995 by the CDF and D0 collaborations at the Tevatron with proton-antiproton data [18, 19], the top quark plays an important role in studying high energy physics. Its Yukawa

interaction is given by

$$\mathcal{L}_{\text{top-Yukawa}} = -\frac{\lambda_t v}{\sqrt{2}} \bar{t}_L t_R - \frac{\lambda_t}{\sqrt{2}} H \bar{t}_L t_R + \text{h.c.}, \quad (1.16)$$

yielding a Yukawa coupling of [6]

$$\lambda_t = \frac{\sqrt{2} m_t}{v} = 0.991 \pm 0.003. \quad (1.17)$$

182 This Yukawa coupling is very large compared to the other Yukawa couplings in the SM ($\mathcal{O}(10^{-2})$),
 183 leading to the belief that the top quark may have an important role in understanding the
 184 mechanism of electroweak symmetry breaking. On top of this, the very short lifetime of the top
 185 quark makes it an excellent candidate to study the properties of a bare quark. Its high mass,
 186 almost 40 times higher than the mass of the closest fermion in mass, leads to a large coupling
 187 with the Higgs boson and makes the top quark an interesting candidate to investigate how
 188 particles acquire mass.

189 The CKM matrix element V_{tb} , given in Equation 1.15, is experimentally found to be much
 190 larger than V_{ts} , V_{td} , and close to unity. The top quark decays through electroweak interactions
 191 since the W boson mass is smaller than the top quark mass and the W boson can be on shell. A
 192 consequence of this is that the top quark has a very short lifetime of only $1/\Gamma_t \approx 5 \cdot 10^{-25}$ s [6]
 193 leading to the fact that the formation of bound states involving top quarks are not allowed.
 194 This lifetime is even shorter than the typical hadronisation timescale of $1/\Lambda_{\text{QCD}} \approx 10^{-23}$ s,
 195 prohibiting gluons to radiate from the top quark and keeping its spin coherent. Since the
 196 electroweak interactions have a vector-axial vector (V-A) coupling structure³, the top quark
 197 spin orientation can be derived from the angular distributions of its decay products. This makes
 198 it possible to study the polarisation of top quarks from the angular distributions in various
 199 processes.

200 The massiveness of the top quark leads to the fact that a large amount of energy is needed to
 201 create one. This is only the case for high energy collisions such as those happening in the Earth's
 202 upper atmosphere when cosmic rays collide with particles in air, or by particle accelerators.
 203 The production of top quarks happens in two ways: single via the electroweak interaction or in
 204 pairs via the strong interaction. At hadron colliders, the dominant production mechanism is top
 205 quark production via gluon ($gg \rightarrow t\bar{t}$) or quark fusion ($q\bar{q} \rightarrow t\bar{t}$). In Figure 1.1, the different top
 206 quark pair production mechanisms are shown. The production channel of gluon fusion is the
 207 main contributor to the top quark pair cross section at the LHC compared to quark fusion at the
 208 Tevatron. The $gg \rightarrow t\bar{t}$ process contributes 80-90% to the total top quark pair cross section in
 209 the LHC centre-of-mass energy regime of 7-14 TeV [6]. In Table 1.5 the predicted top quark
 210 pair production cross sections are given for the LHC and the Tevatron, while in Figure 1.2, a
 211 summary plot of the LHC and Tevatron top quark pair cross section measurements as a function
 212 of the centre-of-mass energy can be found.

213 The singly produced top quarks are produced via the electroweak interaction. These production
 214 mechanisms are subdivided at leading order into three main channels based on the virtuality

³In the SM a vector - axial vector coupling structure ($\gamma^\mu - \gamma^\mu \gamma^5$) is predicted that only permits left-handed fermions or right-handed anti fermions to interact with a spin-1 particle.

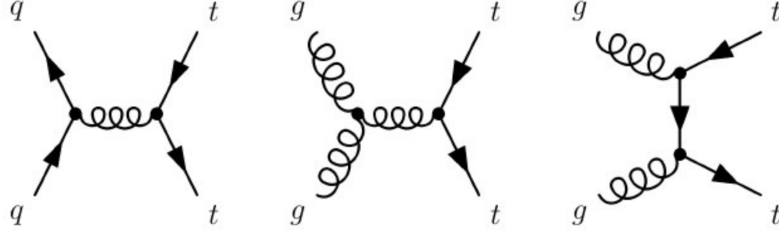


Figure 1.1: Leading order diagrams of the top quark pair production. Gluon fusion (right and middle) are the dominant processes at the LHC, while quark fusion (left) is the dominant one at the Tevatron.

Table 1.5: Predictions on the top quark pair production cross sections at next-to-next-to-leading order with next-to-next-to-leading log soft gluon resummation per centre-of-mass energy [6]. The first uncertainty is from scale dependence, while the second uncertainty originates from parton density functions.

Experiment	Top quark mass	Centre-of-mass energy	Cross section (pb)
Tevatron	$m_t = 173.3$ GeV	$\sqrt{s} = 1.96$ TeV	$\sigma_{t\bar{t}} = 7.16^{+0.11+0.17}_{-0.20-0.12}$
LHC	$m_t = 173.2$ GeV	$\sqrt{s} = 7$ TeV	$\sigma_{t\bar{t}} = 173.6^{+4.5+8.9}_{-5.9-8.9}$
LHC	$m_t = 173.2$ GeV	$\sqrt{s} = 8$ TeV	$\sigma_{t\bar{t}} = 247.7^{+6.3+11.5}_{-8.5-11.5}$
LHC	$m_t = 173.2$ GeV	$\sqrt{s} = 13$ TeV	$\sigma_{t\bar{t}} = 816.0^{+19.4+34.4}_{-28.6-34.4}$

215 ($Q^2 = -p_\mu p^\mu$) of the exchanged W boson. In Figure 1.3, the corresponding Feynman diagrams
 216 are shown. The single top quark production cross sections, given in Table 1.6, are smaller than
 217 the top quark pair production cross sections since the electroweak coupling strength is smaller
 218 than the strong coupling strength. In addition, for the single top quark production, there is the
 219 need of sea quarks (b, \bar{q}) in the initial states for which the parton density functions increase
 220 less steeply at low momentum fractions compared to the gluon parton density functions.

221 The production via the t -channel has a virtuality of the W boson $Q^2 > 0$, making it space-like.
 222 It is produced via the scattering of the W boson of a bottom quark coming from a proton
 223 or from gluon splitting ($g \rightarrow b\bar{b}$). It has the highest single top quark cross section in proton
 224 collisions and the top quark production is roughly twice as large than the antitop quark. This is
 225 a consequence of the up-down valence quark composition of the proton. This feature makes the
 226 t -channel sensitive to the parton density functions of the proton. The s -channel is the production
 227 mechanism with the smallest cross section. Here the W boson is time-like ($Q^2 < 0$) which
 228 requires the W boson to have a large virtuality to produce the heavier top quark. It is produced
 229 from two quarks belonging to the same isodoublet (e.g. $u\bar{d}$) and subsequently decays to $t\bar{b}$.
 230 This process gets enhanced by many beyond the Standard Model scenarios via the addition of
 231 new heavy particles such as W' . The tW -channel has a top quark produced in association with a
 232 W boson produced on shell $Q^2 = -m_W^2$. This mode is negligible at the Tevatron, but of relevant
 233 size at the LHC. The tW -channel is sensitive to new physics affecting the Wtb vertex. The single
 234 top quark production cross section measurements by the CMS collaboration can be found in
 235 Figure 1.4.

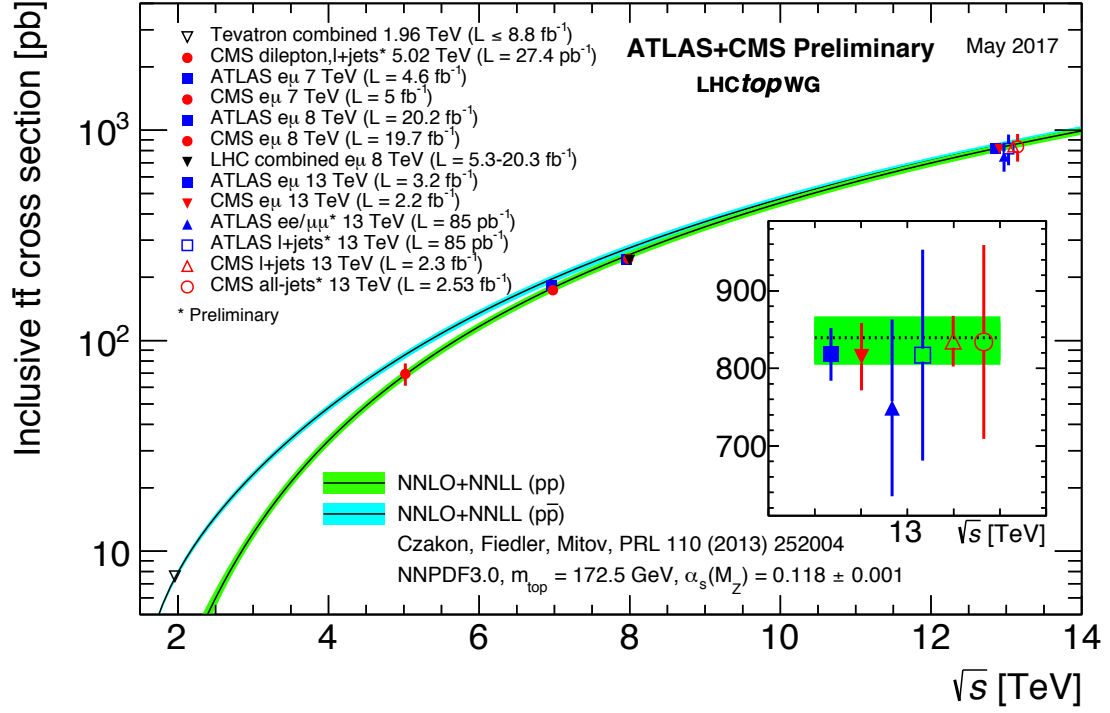


Figure 1.2: Summary of the LHC and the Tevatron measurements of the top quark pair production cross section as function of the centre-of-mass energy compared with the next-to-next-to-leading order QCD calculation. The theory bands are the uncertainties due to renormalization and factorisation scales, parton density functions and the strong coupling. The mass of the top quark is assumed to be 172.5 GeV. Measurements for the same centre-of-mass energy are slightly off-set for clarity. Figure taken from [20].

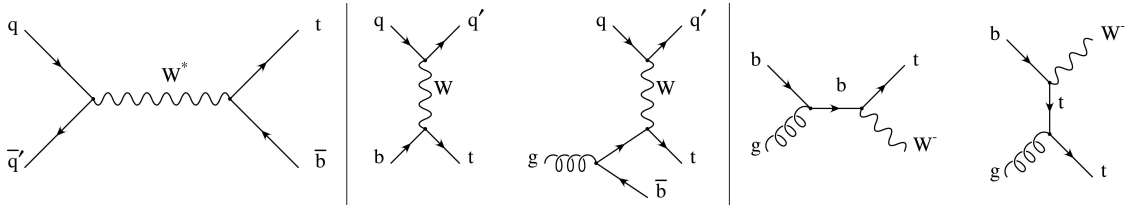


Figure 1.3: Leading order Feynman diagrams of the electroweak production of single top quarks in the s -channel (left), t -channel (middle), and for the tW associated production. Figure taken from [21].

Table 1.6: Predictions on the single top quark production cross sections at next-to-leading order per centre-of-mass energy [6]. The uncertainties from scale dependence and from parton density functions are combined in quadrature or given separately (scale + PDF). For the t -channel the relative proportions to t and \bar{t} are 65% and 35%. For the s -channel this is respectively 69% and 31%. The $t\bar{W}$ -channel has an equal proportion of top and antitop quarks. For Tevatron, the top quark mass is assumed to be 173.3 GeV, while the LHC predictions use $m_t = 172.5$ GeV [6, 22].

Collider	Centre-of-mass energy	Cross section $\sigma_{t+\bar{t}}$ (pb)		
		t -channel	s -channel	$t\bar{W}$ -channel
Tevatron	$\sqrt{s} = 1.96$ TeV	$2.06^{+0.13}_{-0.13}$	$1.03^{+0.05}_{-0.05}$	-
LHC	$\sqrt{s} = 7$ TeV	$63.89^{+2.91}_{-2.52}$	$4.29^{+0.19}_{-0.17}$	$15.74^{+0.40+1.10}_{-0.40-1.14}$
LHC	$\sqrt{s} = 8$ TeV	$84.69^{+3.76}_{-3.23}$	$5.24^{+0.22}_{-0.20}$	$22.37^{+0.60+1.40}_{-0.60-1.40}$
LHC	$\sqrt{s} = 13$ TeV	$216.99^{+9.04}_{-7.71}$	$10.32^{+0.40}_{-0.36}$	$71.7^{+1.80+3.40}_{-1.80-3.40}$

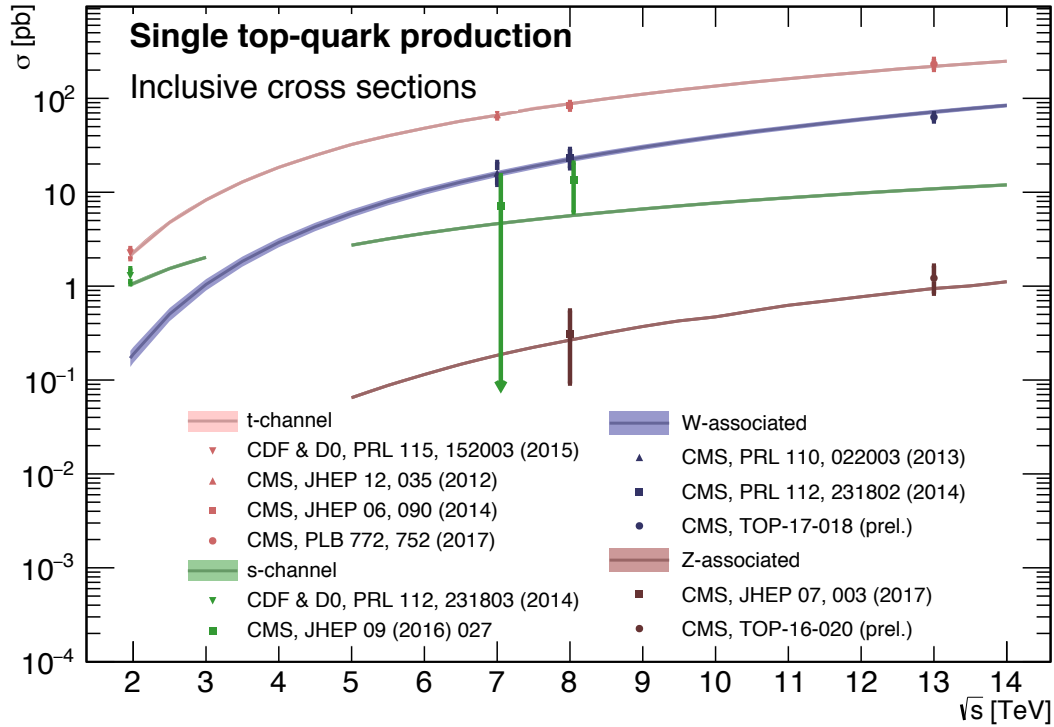


Figure 1.4: Summary of the measurements of the single top quark production cross section as function of the centre-of-mass energy. Figure taken from [23].

1.5 Effective field theories

Problems can be simplified if one looks at the relevant scale of the process that one want to investigate, for example the chemical properties of an hydrogen atom can be described without any knowledge of quark interactions inside the proton. In this case, the proton can be considered the elementary object (indivisible) due to the fact that the binding energy of the constituents is much bigger than the energy of the electron in orbit around the proton. Effective field theories are based on this kind of separation of different energy scales in a system [24]. Effective field theories can be used for theories where the perturbative expansion cannot be trusted, e.g. QCD at low energy, or as bottom up approach to look for new physics in a model independent way. The latter is the way effective field theory will be used throughout this thesis.

The main idea behind effective field theory is easily explained via the example of the Fermi theory. Fermi explained in 1933 [25] the β -decay as a product of currents:

$$\mathcal{L}_{\text{EFT}}^{\text{Fermi}} = -\frac{G_F}{\sqrt{2}} J^\mu J_\mu^\dagger, \quad (1.18)$$

where G_F is the Fermi coupling constant, measured to be $G_F \approx 1.17 \times 10^{-5} \text{ GeV}^{-2}$. The current J_μ can be written as the sum of an hadronic J_μ^h and leptonic J_μ^l current, where for simplicity only the leptonic current is discussed.

$$J_\mu^l = \sum_i \bar{\nu}_i \gamma_\mu (1 - \gamma_5) l_i. \quad (1.19)$$

Historically, charged currents were flavour universal and the later discovered parity violation of the weak interaction led to the V-A structure. After this, the $\text{SU}(2)_L$ symmetry was postulated and the existence of neutral currents was predicted. The effective Lagrangian used then (given in Equation 1.18), could nowadays be build starting from $\text{SU}(2)_L$ symmetries only.

The muon decay can be computed from two different starting points. The effective Fermi Lagrangian provides the decay width of the muon into an electron and two neutrinos

$$\Gamma(\mu \rightarrow e \bar{\nu}_e \nu_\mu) \approx \frac{1}{96\pi^3} \frac{m_\mu^2}{\Lambda_F^4}, \quad (1.20)$$

where Λ_F is the energy scale defined as

$$\frac{G_F}{\sqrt{2}} = \frac{1}{\Lambda_F^2}. \quad (1.21)$$

From muon decay measurements, the value of Λ_F is determined to be $\Lambda_F \approx 348 \text{ GeV}$ [24]. From the SM Lagrangian, one could also calculate the muon decay. Considering that the momenta involved are small compared to the W boson mass, the propagator's denominator can be expanded as [1]

$$\frac{1}{p^2 - m_W^2} = -\frac{1}{m_W^2} - \frac{p^2}{m_W^4} + \dots \quad (1.22)$$

Looking at the first term, and identifying

$$\frac{g^2}{8m_W} = \frac{1}{\Lambda_F^2}, \quad (1.23)$$

one sees that this corresponds with Equation 1.20, thus the effective Lagrangian in Equation 1.18 is the first term of the expansion in $\frac{1}{m_W^2}$ applied on the full Lagrangian.

An effective theory is thus a Taylor expansion in the ratio of two scales and the only remnants of the full theory at low energies are the symmetries and the values of the coupling constants. If the expansion parameter is small, one can truncate the series leading to the Lagrangian containing a finite number of free coefficients, making predictions possible. The error on these predictions is then of the order as the truncated piece.

The SM can be seen as an effective theory applicable up to energies not exceeding a scale Λ . Therefore, remnants should still be valid and the theory above that scale should have a gauge group containing $SU(3)_C \times SU(2)_L \times U(1)_Y$ and all the SM degrees of freedom, as well as reduce to the SM at lower energies. The general SM Lagrangian becomes then

$$\mathcal{L}_{\text{SM+EFT}} = \mathcal{L}_{\text{SM}}^{(4)} + \frac{1}{\Lambda} \sum_k C_k^{(5)} Q_k^{(5)} + \frac{1}{\Lambda^2} \sum_k C_k^{(6)} Q_k^{(6)} + \mathcal{O}\left(\frac{1}{\Lambda^3}\right), \quad (1.24)$$

where $Q_k^{(n)}$ are dimension- n operators (currents) and $C_k^{(n)}$ the corresponding dimensionless coupling constants, so-called Wilson coefficients. The Wilson coefficients are determined by the underlying high energy theory.

In the Warsaw basis [26], a set of independent operators of dimension 5 and 6 are built out of the SM fields and are consistent with the SM gauge symmetries and is fully derived in Ref. [26]. In general the various measurements show a good agreement with the SM predictions and by lack of deviations from the SM, limits on the anomalous couplings can be derived. The estimated coupling strengths per operator contributing to single top quark production obtained from various measurements at the LHC and Tevatron are shown in Figure 1.5 for which the conventions are discussed in Ref. [27]. These results are consistent with the SM expectation for which those operators vanish.

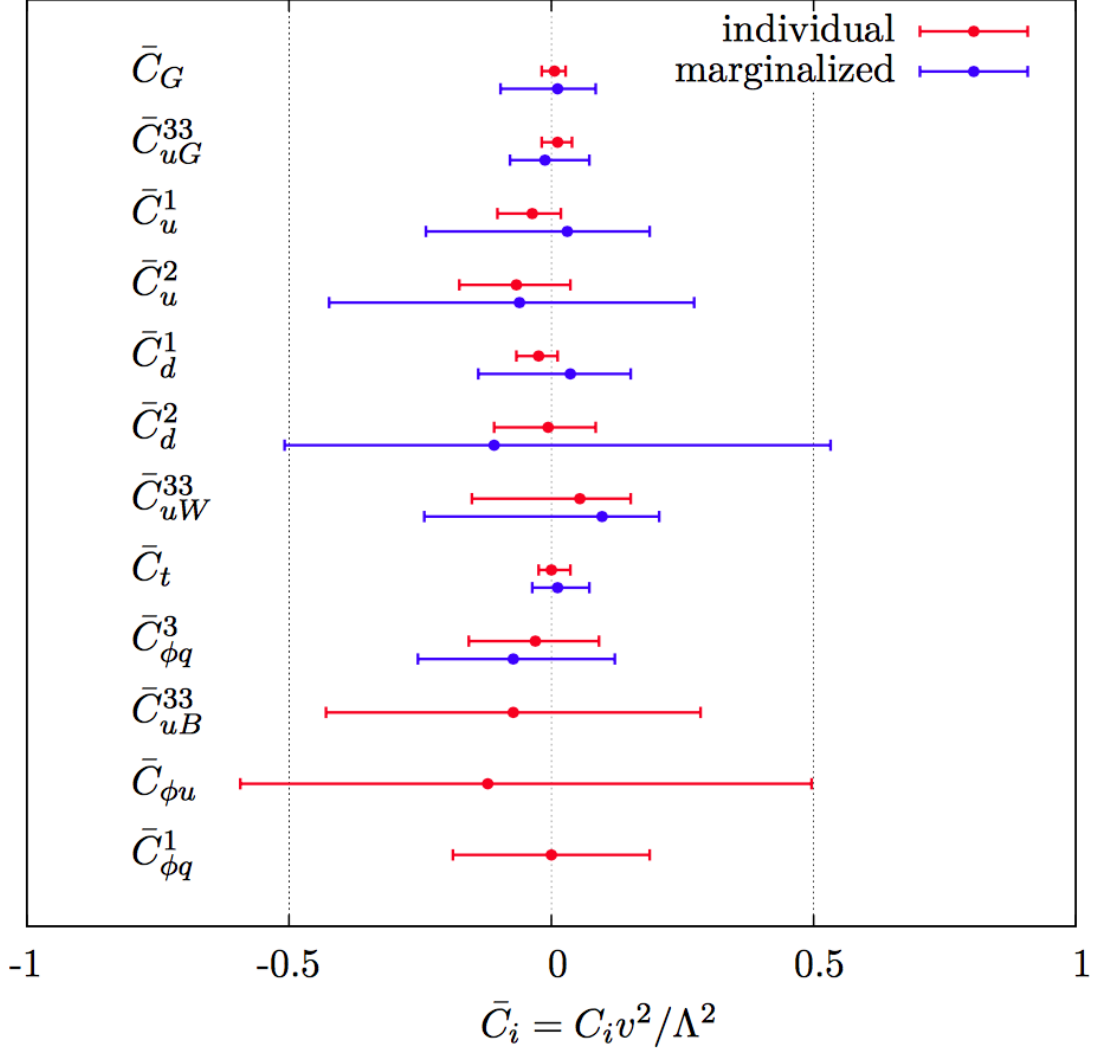


Figure 1.5: Global fit results of top quark effective field theory to experimental data including all constrained operators at dimension six. For the operators, the Warsaw basis of [26] is used. The bounds are set on the Wilson coefficients of various operators contributing to top quark production and decay in two cases (red) all other coefficients set to zero, or (blue) all other coefficients are marginalised over. Figure taken from [28].

1.6 Motivation for new physics

Many high energy experiments confirm the success of the SM. In particular the scalar boson, the cornerstone of the SM, has consecrated the theory. Unfortunately there are also strong indications that the SM ought to be a lower energy expression of a more global theory. The existence of physics beyond the SM (BSM) [29] is strongly motivated. These motivations are based on direct evidence from observation such as the existence of neutrino masses, the existence of dark matter and dark energy, or the matter-antimatter asymmetry, and also from theoretical problems such as the hierarchy problem, the coupling unification or the large numbers of free parameters in the SM.

In the SM, the neutrinos are assumed to be massless, while experiments with solar, atmospheric, reactor and accelerator neutrinos have established that neutrinos can oscillate and change flavour during flight [4, 5]. These oscillations are only possible when neutrinos have masses. The flavour neutrinos (ν_e , ν_μ , ν_τ) are then linear expressions of the fields of at least three mass eigenstate neutrinos ν_1 , ν_2 , and ν_3 .

The ordinary or baryonic matter described by the SM describes only 5% of the mass (energy) content of the universe. Astrophysical evidence indicated that dark matter is contributing to approximately 27% and dark energy to 68% of the content of the universe. From the measurements of the temperature and polarizations anisotropies of the cosmic microwave background by the Planck experiment [30], the density of cold non baryonic matter is determined. Cold dark matter is assumed to be only sensitive to the weak and gravitational force, leading to only one possible SM candidate: the neutrino. However, these are too light to account for the vast amount of dark matter and other models are needed. Dark energy is assumed to be responsible for the acceleration in the expansion of the universe [31].

At the Big Bang, matter and antimatter are assumed to be produced in equal quantities. However, it is clear that we are surrounded by matter. So where did all the antimatter go? In 1967, Sakharov identified three mechanisms that are necessary to obtain a global matter antimatter asymmetry [32]. These mechanisms are those of baryon and lepton number violation, that at a given moment in time there was a thermal imbalance for the interactions in the universe, and there is charge C and charge parity CP violation⁴.

The large number of free parameters in the SM comes from the nine fermion masses, three CKM mixing angles and one CP violating phase, one EM coupling constant g' , one weak coupling constant g , one strong coupling constant g_s , one QCD vacuum angle, one vacuum expectation value, and one mass of the scalar boson. This large number of free parameters leads to the expectation of a more elegant and profound theory beyond the SM.

The hierarchy problem [33] is related to the huge difference in energy between the weak scale and the Planck scale. The vev of the Brout-Englert-Higgs field determines the weak scale that is approximately 246 GeV. The radiative corrections to the scalar boson squared mass m_H^2 , coming from its self couplings and couplings to fermions and gauge bosons, are quadratically

⁴The rate of a process $i \rightarrow f$ can be different from the CP-conjugate process: $\bar{i} \rightarrow \bar{f}$. The SM includes sources of CP-violation through the residual phase of the CKM matrix. However, these could not account for the magnitude of the asymmetry observed.

proportional to the ultraviolet momentum cut-off Λ_{UV} . This cut-off is at least equal to the energy to which the SM is valid without the need of new physics. For the SM to be valid up to the Planck mass, the correction to m_H^2 becomes thirty orders of magnitude larger than m_H^2 . This implies that an extraordinary cancellation of terms should happen. This is also known as the naturalness problem of the H boson mass.

The correction to the squared mass of the scalar boson coming from a fermion f , coupling to the scalar field ϕ with a coupling λ_f is given by

$$\Delta m_H^2 = -\frac{|\lambda_f|^2}{8\pi^2} \Lambda_{UV}^2, \quad (1.25)$$

while the correction to the mass from a scalar particle S with a mass m_S , coupling to the scalar field with a Lagrangian term $-\lambda_S|\phi|^2|S|^2$ is

$$\Delta m_H^2 = \frac{|\lambda_S|^2}{16\pi^2} \left(\Lambda_{UV}^2 - 2m_S^2 \ln \left(\frac{\Lambda_{UV}}{m_S} \right) + \dots \right). \quad (1.26)$$

As one can see the correction term to m_H^2 is much larger than m_H^2 itself. By introducing BSM physics models that introduce new scalar particles at the TeV scale that couple to the scalar boson one can cancel the Λ_{UV}^2 divergence and avoid this fine-tuning.

The choice of the $SU(3)_C \times SU(2)_L \times U(1)_Y$ symmetry group itself as well as the separate treatment of the three forces included in the SM raises concern. The intensity of the forces show a large disparity around the electroweak scale, but have comparable strengths at higher energies. The electromagnetic and weak forces are unified in a electroweak interaction, but the strong coupling constant does not encounter the other coupling constants at high energies. In order to reach a grand unification, the running of couplings can be modified by the addition of new particles in BSM models.

1.7 An effective approach beyond the SM: FCNC involving a top quark

The closeness of the top quark mass to the electroweak scale led physicists to believe that it is a sensitive probe for new physics. Studying its properties is therefore an important topic of the experimental program at the LHC. Several extensions of the SM enhance the FCNC branching fractions and can be probed at the LHC [17], from which some of them are shown in Table 1.7. Previous searches have been performed at the Tevatron by the CDF [34] and D0 [35] collaborations, and at the LHC by the ATLAS [36–40] and CMS [41–45] collaborations.

The impact of BSM models can be written in a model independent way by means of an effective field theory valid up to an energy scale Λ . The leading effects are parametrized by a set of fully gauge symmetric operators that are added to the SM Lagrangian and can be reduced to a minimal set of operators as seen in Equation 1.24. For simplicity, the assumption is made that new physics effects are exclusively described by dimension-6 operators, thus neglecting

Table 1.7: The predicted branching fractions \mathcal{B} for FCNC interactions involving the top quark in some BSM models [17]: quark singlet (QS), generic two Higgs doublet model (2HDM) and the minimal supersymmetric extensions to the SM (MSSM);

Process	QS	2HDM	MSSM	Process	QS	2HDM	MSSM
$t \rightarrow uZ$	$\leq 1.1 \times 10^{-4}$	—	$\leq 2 \times 10^{-6}$	$t \rightarrow cZ$	$\leq 1.1 \times 10^{-4}$	$\leq 10^{-7}$	$\leq 2 \times 10^{-6}$
$t \rightarrow u\gamma$	$\leq 7.5 \times 10^{-9}$	—	$\leq 2 \times 10^{-6}$	$t \rightarrow c\gamma$	$\leq 7.5 \times 10^{-9}$	$\leq 10^{-6}$	$\leq 2 \times 10^{-6}$
$t \rightarrow ug$	$\leq 1.5 \times 10^{-7}$	—	$\leq 8 \times 10^{-5}$	$t \rightarrow cg$	$\leq 1.5 \times 10^{-7}$	$\leq 10^{-4}$	$\leq 8 \times 10^{-5}$
$t \rightarrow uH$	$\leq 4.1 \times 10^{-5}$	$\leq 5.5 \times 10^{-6}$	$\leq 10^{-5}$	$t \rightarrow cH$	$\leq 4.1 \times 10^{-5}$	$\leq 10^{-3}$	$\leq 10^{-5}$

334 neutrino physics. In the fully gauge symmetric case, the EFT Lagrangian is then given by

$$\mathcal{L}_{\text{SM+EFT}} = \mathcal{L}_{\text{SM}} + \sum_i \frac{\bar{c}_i}{\Lambda^2} O_i + \mathcal{O}\left(\frac{1}{\Lambda^3}\right), \quad (1.27)$$

where the Wilson coefficients \bar{c}_i depend on the considered theory and on the way that new physics couples to the SM particles. Taking into account that Λ is large, contributions suppressed by powers of Λ greater than two are neglected. Additionally, all four fermion operators are omitted for the rest of this thesis. The Warsaw basis is adopted for the independent effective operators [26], parametrising the new physics effects relevant for the flavour changing neutral current interactions of the top quark as, all flavour indices understood,

$$\begin{aligned} \mathcal{L}_{\text{EFT}}^t = & \frac{\bar{c}_{uG}}{\Lambda^2} \Phi^\dagger \cdot [\bar{Q}_L \sigma^{\mu\nu} \mathcal{T}_a u_R] G_{\mu\nu}^a + \frac{\bar{c}_{uB}}{\Lambda^2} \Phi^\dagger \cdot [\bar{Q}_L \sigma^{\mu\nu} u_R] B_{\mu\nu} + \frac{2\bar{c}_{uW}}{\Lambda^2} \Phi^\dagger T_i \cdot [\bar{Q}_L \sigma^{\mu\nu} u_R] W_{\mu\nu}^i \\ & + i \frac{\bar{c}_{hu}}{\Lambda^2} \left[\Phi^\dagger \overleftrightarrow{D}_\mu \Phi \right] [\bar{u}_R \gamma^\mu u_R] + i \frac{\bar{c}_{hq}^{(1)}}{\Lambda^2} \left[\Phi^\dagger \overleftrightarrow{D}_\mu \Phi \right] [\bar{Q}_L \gamma^\mu Q_L] \\ & + i \frac{4\bar{c}_{Hq}^{(3)}}{\Lambda^2} \left[\Phi^\dagger T_i \overleftrightarrow{D}_\mu \Phi \right] [\bar{Q}_L \gamma^\mu T^i Q_L] + \frac{\bar{c}_{uh}}{\Lambda^2} \Phi^\dagger \Phi \Phi^\dagger \cdot [\bar{Q}_L u_R] + \text{h.c.}, \end{aligned} \quad (1.28)$$

where the left handed $SU(2)_L$ doublet of the quark fields is denoted by Q_L , the up-type right handed fields by u_R , the down-type right handed fields by d_R , the $SU(2)_L$ doublet of the Higgs field by Φ , the field strength tensors as

$$\begin{aligned} B_{\mu\nu} &= \partial_\mu B_\nu - \partial_\nu B_\mu, \\ W_{\mu\nu}^k &= \partial_\mu W_\nu^k - \partial_\nu W_\mu^k - g \epsilon_{ij}^k W_\mu^i W_\nu^j, \\ G_{\mu\nu} &= \partial_\mu G_\nu^a - \partial_\nu G_\mu^a + g_s f_{bc}^a G_\mu^b G_\nu^c, \end{aligned} \quad (1.29)$$

denoting the structure constant of the $SU(3)_C$ group as f_{bc}^a and the structure constant of the $SU(2)_L$ group as ϵ_{ij}^k . The gauge covariant derivatives are also standard defined as

$$D_\mu \Phi = \partial_\mu \Phi - \frac{1}{2} i g' B_\mu \Phi - i g T_k W_\mu^k \Phi \quad (1.30)$$

with the conventions of Section 1.2. The representation matrices T of $SU(2)_L$ are defined in Equation 1.1, while the representation matrices \mathcal{T} of $SU(3)_C$ are the Gell-Mann matrices [1].

The hermitian derivative operator is defined as

$$\Phi^\dagger \overleftrightarrow{D} \Phi = \Phi^\dagger D^\mu \Phi - D_\mu \Phi^\dagger \Phi. \quad (1.31)$$

After electroweak symmetry breaking, the operators induce [17, 46] both corrections to the SM couplings and new interactions at tree level such as FCNC interactions. The FCNC interactions of the top quark that are not present in the SM are given by

$$\mathcal{L}_{\text{EFT}}^t = \frac{\sqrt{2}}{2} \sum_{q=u,c} \left[g' \frac{\kappa_{t\gamma q}}{\Lambda} A_{\mu\nu} \bar{t} \sigma^{\mu\nu} (f_{\gamma q}^L P_L + f_{\gamma q}^R P_R) q \right. \quad (1.32)$$

$$\left. + \frac{g}{2\cos\theta_W} \frac{\kappa_{tZq}}{\Lambda} Z_{\mu\nu} \bar{t} \sigma^{\mu\nu} (f_{Zq}^L P_L + f_{Zq}^R P_R) q \right. \quad (1.33)$$

$$\left. + \frac{\sqrt{2}g}{4\cos\theta_W} \zeta_{tZq} \bar{t} \gamma^\mu (\tilde{f}_q^L P_L + \tilde{f}_q^R P_R) q Z_\mu \right. \quad (1.34)$$

$$\left. + g_s \frac{\kappa_{tgq}}{\Lambda} Z_{\mu\nu} \bar{t} \sigma^{\mu\nu} (f_{gq}^L P_L + f_{gq}^R P_R) q G_{\mu\nu}^a \right. \quad (1.35)$$

$$\left. + \eta_{Hqt} \bar{t} (\hat{f}_q^L P_L + \hat{f}_q^R P_R) q H + \text{h.c.} \right], \quad (1.36)$$

where the value of the FCNC couplings at scale Λ are represented by $\kappa_{tZq}, \kappa_{tgq}, \kappa_{t\gamma q}, \zeta_{tZq}$, and η_{Hqt} . These are assumed to be real and positive, with the unit of GeV^{-1} for $\kappa_{t\gamma q}/\Lambda$ and no unit for ζ_{tZq} and η_{Hqt} . In the equation $\sigma^{\mu\nu}$ equals to $\frac{i}{2} [\gamma^\mu, \gamma^\nu]$, and the left- and right-handed chirality projector operators are denoted by P_L and P_R . The electromagnetic coupling constant is denoted by g' , the strong interaction coupling is denoted as g_s , while the electroweak interaction is parametrised by the coupling constant g and the electroweak mixing angle θ_W . The complex chiral parameters are normalized according to $|f_{xq}^L|^2 + |f_{xq}^R|^2 = 1$, $|\tilde{f}_q^L|^2 + |\tilde{f}_q^R|^2 = 1$, and $|\hat{f}_q^L|^2 + |\hat{f}_q^R|^2 = 1$. In the expression for $\mathcal{L}_{\text{EFT}}^t$, the unitary gauge is adopted and the scalar field is expanded around its vacuum expectation value v with H being the SM scalar boson. The field strength tensors of the photon A_μ , the gluon field $G_{\mu}^{1\dots 8}$, and the Z boson Z_μ^0 are defined as

$$\begin{aligned} A_{\mu\nu} &= \partial_\mu A_\nu - \partial_\nu A_\mu, \\ Z_{\mu\nu} &= \partial_\mu Z_\nu - \partial_\nu Z_\mu, \text{ and} \\ G_{\mu\nu} &= \partial_\mu G_\nu^a - \partial_\nu G_\mu^a + g_s f_{bc}^a G_\mu^b G_\nu^c. \end{aligned} \quad (1.37)$$

335 Note that there are two coupling constants arising in $\mathcal{L}_{\text{EFT}}^t$, which is a residue of electroweak
 336 symmetry breaking. The massive Z boson will appear in both the Z_μ^0 field as well as the covariant
 337 derivative, leading to an extra Z-vertex.

338 The relations between the Wilson coefficients in (1.28) and the coupling strengths of the
 339 interactions in Equation 1.36 can be derived. The 14 effective operators are mapped onto 10
 340 free parameters providing a more minimal parametrisation of the anomalous interactions of the
 341 top quark.

$$\begin{aligned}
 \kappa_{t\bar{g}q} f_{gq}^L &= \frac{v}{g_s \Lambda} [\bar{c}_{uG}]_{i3}^* , & \kappa_{t\bar{g}q} f_{gq}^R &= \frac{v}{g_s \Lambda} [\bar{c}_{uG}]_{3i} , \\
 \kappa_{t\gamma q} f_{\gamma q}^L &= \frac{v}{g' \Lambda} [\cos \theta_W \bar{c}_{uB} - \sin \theta_W \bar{c}_{uW}]_{i3}^* , & \kappa_{t\gamma q} f_{\gamma q}^R &= \frac{v}{g' \Lambda} [\sin \theta_W \bar{c}_{uB} - \cos \theta_W \bar{c}_{uW}]_{3i} , \\
 \kappa_{tZq} f_{Zq}^L &= -\frac{2\cos \theta_W v}{g \Lambda} [\sin \theta_W \bar{c}_{uB} + \cos \theta_W \bar{c}_{uW}]_{i3}^* , & \kappa_{tZq} f_{Zq}^R &= -\frac{2\cos \theta_W v}{g \Lambda} [\cos \theta_W \bar{c}_{uB} + \sin \theta_W \bar{c}_{uW}]_{3i} , \\
 \zeta_{tZq} \tilde{f}_{Zq}^L &= -\frac{2v^2}{\Lambda^2} [(\bar{c}_{hq}^{(1)} - \bar{c}_{hq}^{(3)})_{i3} + (\bar{c}_{hq}^{(1)} - \bar{c}_{hq}^{(3)})_{3i}^*] , & \zeta_{tZq} \tilde{f}_{Zq}^R &= -\frac{2v^2}{\Lambda^2} [(\bar{c}_{hu})_{i3} + (\bar{c}_{hu})_{3i}^*] , \\
 \eta_{tHq} \hat{f}_{Hq}^L &= \frac{3v^2}{2\Lambda^2} [\bar{c}_{uh}]_{3i}^* , & \eta_{tHq} \hat{f}_{Hq}^R &= \frac{3v^2}{2\Lambda^2} [\bar{c}_{uh}]_{i3} .
 \end{aligned} \tag{1.38}$$

342 1.8 Experimental constraints on top-FCNC

Experiments commonly put limits on the branching fractions which allow an easier interpretation across different EFT models by use of the branching fraction

$$\mathcal{B}(t \rightarrow qX) = \frac{\delta_{tXq}^2 \Gamma_{t \rightarrow qX}}{\Gamma_t} , \tag{1.39}$$

343 where $\Gamma_{t \rightarrow qX}$ represents the FCNC decay width⁵ for a coupling strength $\delta_{tXq}^2 = 1$, and Γ_t the full
 344 decay width of the top quark. In the SM, supposing a top quark mass of 172.5 GeV, the full
 345 width becomes $\Gamma_t^{\text{SM}} = 1.32$ GeV [47].

346 Searches for top-FCNC usually adopt a search strategy depending on the experimental set-up
 347 and the FCNC interaction of interest, looking either for FCNC interactions in the production of a
 348 single top quark or in its decay for top quark pair interactions. In Figure 1.6, these two cases
 349 are shown for the tZq vertex.

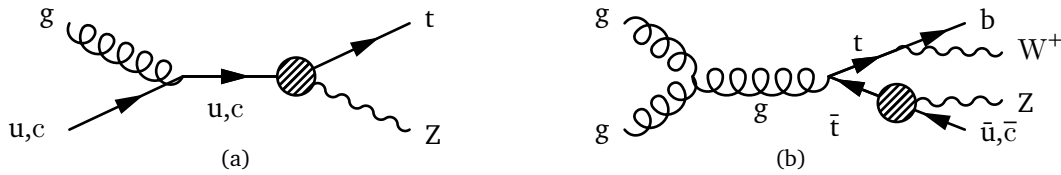


Figure 1.6: Feynman diagrams for the processes with a tZq FCNC interaction, where the FCNC interaction is indicated with the shaded dot. (a) Single top quark production through an FCNC interaction. (b) Top quark pair production with an FCNC induced decay.

⁵The decay width of a certain process represents the probability per unit time that a particle will decay. The total decay width, defined as the sum of all possible decay widths of a particle, is inversely proportional to its lifetime.

351 The observation of top-FCNC interactions has yet to come and experiments have so far only
 352 been able to put upper bounds on the branching fractions. An overview of the best current limits
 353 is given in Table 1.8. In Figure 1.7 a comparison is shown between the current best limits set by
 354 ATLAS and CMS with respect to several BSM model benchmark predictions. From there one can
 355 see that FCNC searches involving a Z or H boson are close to excluding or confirming several
 356 BSM theories. In Figure 1.9, the searches performed by CMS are summarised. For the tZq
 357 vertex, the best limit from CMS comes from Ref. [41] where both single top quark and top quark
 358 pair are studied. The observed (expected) limits 95% CL at 8 TeV for the FCNC tZq interaction
 359 by CMS are $\mathcal{B}(t \rightarrow uZ) < 2.2 \times 10^{-4} (2.7 \times 10^{-4})$ and $\mathcal{B}(t \rightarrow cZ) < 4.9 \times 10^{-4} (12 \times 10^{-4})$. In
 360 Figure 1.8, the summary of the 95% confidence level observed limits on the branching fractions
 361 of the top quark decays to a charm or up quark and a neutral boson is given, considering the
 results from the HERA, the LEP, the Tevatron, and the LHC.

Table 1.8: Overview of the most stringent observed and expected experimental limits on top-FCNC branching fractions \mathcal{B} at 95% confidence level.

Process	Search mode	Observed \mathcal{B}	Expected \mathcal{B}	Experiment
$t \rightarrow uZ$	top quark pair decay	1.7×10^{-4}	2.4×10^{-4}	ATLAS [40]
$t \rightarrow u\gamma$	single top quark production	1.3×10^{-4}	1.9×10^{-4}	CMS [43]
$t \rightarrow ug$	single top quark production	4.0×10^{-5}	3.5×10^{-5}	ATLAS [37]
$t \rightarrow uH$	top quark pair decay	2.4×10^{-3}	1.7×10^{-3}	ATLAS [39]
$t \rightarrow cZ$	top quark pair decay	2.3×10^{-4}	3.2×10^{-4}	ATLAS [40]
$t \rightarrow c\gamma$	single top quark production	2.0×10^{-3}	1.7×10^{-3}	CMS [43]
$t \rightarrow cg$	single top quark production	2.0×10^{-4}	1.8×10^{-4}	ATLAS [37]
$t \rightarrow cH$	top quark pair decay	2.2×10^{-3}	1.6×10^{-3}	CMS [39]

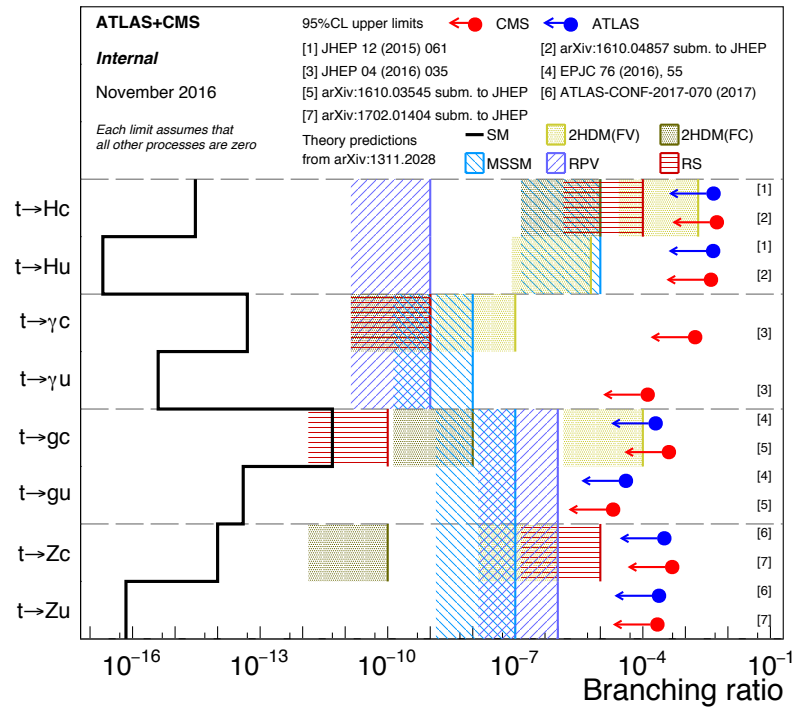


Figure 1.7: Current best limits set by CMS and ATLAS for top-FCNC interactions. Figure adapted from [23].

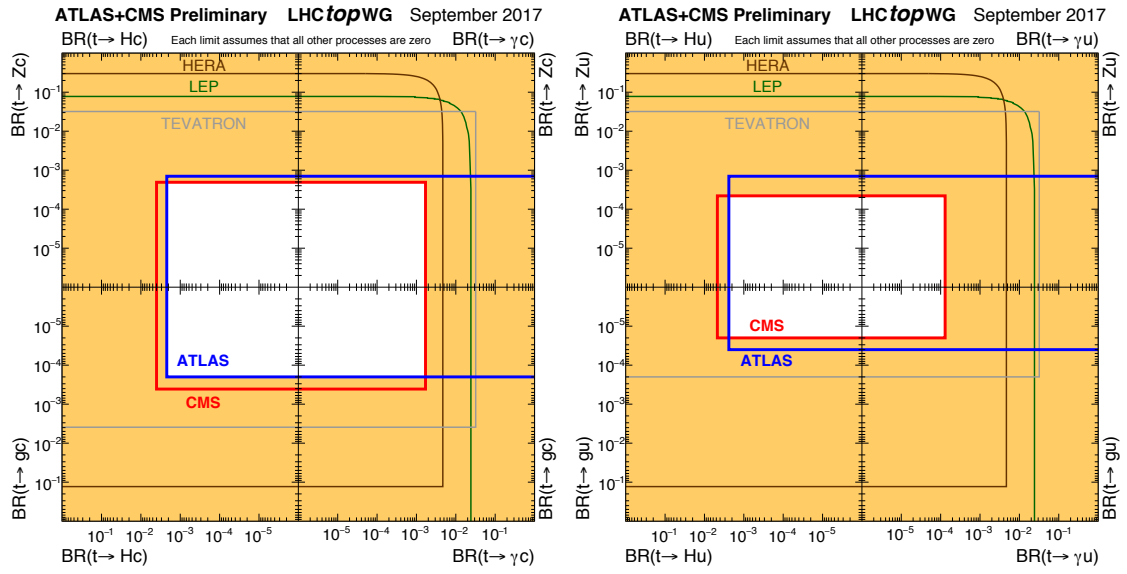


Figure 1.8: Summary of the current 95% confidence level observed limits on the branching fractions of the top quark decays via flavour changing neutral currents to a charm (left) or up (right) quark and a neutral boson. The coloured lines represent the results from HERA (the most stringent limits between the ones obtained by the H1 and ZEUS collaborations, in brown), LEP (combined ALEPH, DELPHI, L3 and OPAL collaborations result, in green), TEVATRON (the most stringent limits between the ones obtained by the CDF and D0 collaborations, in grey). The yellow area represents the region excluded by the ATLAS and the CMS Collaborations. Figure taken from [20].

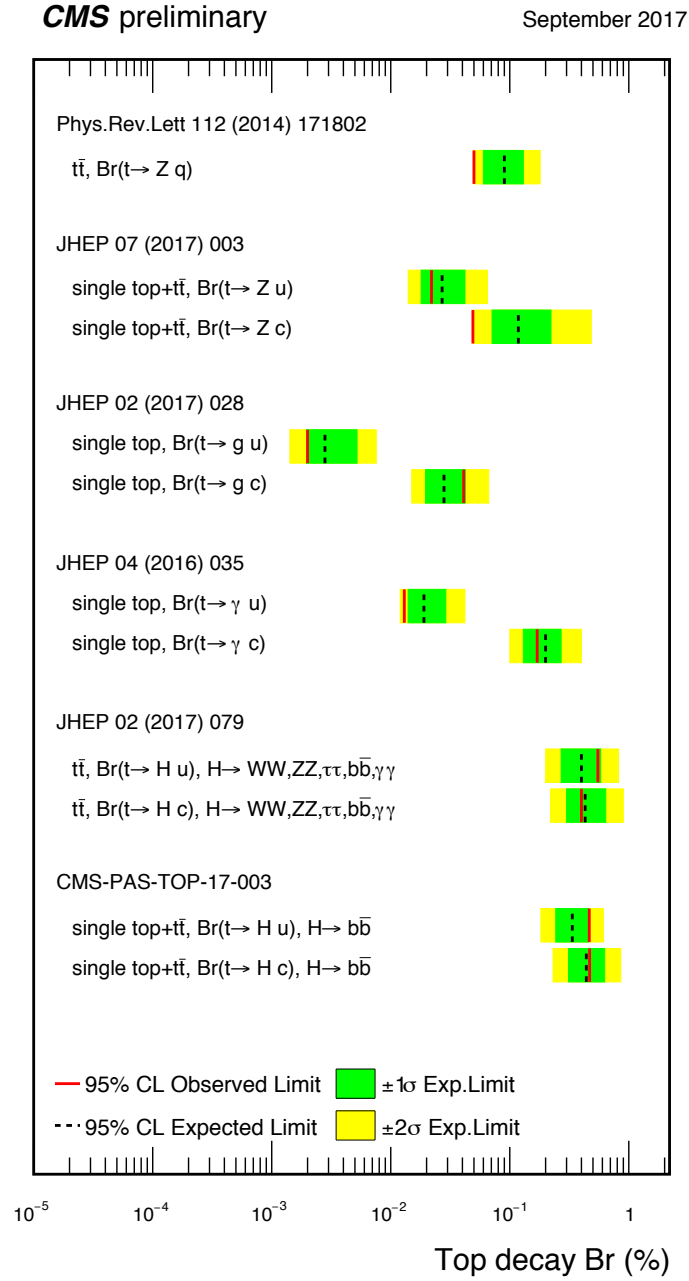


Figure 1.9: Summary of the FCNC branching fractions from CMS searches at 8 TeV. Figure taken from [23].